Synthesis and Electrochemistry of Li- and Na-Fulleride Doped Mesoporous Ta Oxides

Boris O. Skadtchenko,[†] Michel Trudeau,[‡] Chai-Won Kwon,[§] Bruce Dunn,[§] and David Antonelli*,[†]

Department of Chemistry and Biochemistry, University of Windsor, 401 Sunset Avenue, Windsor, Ontario, Canada N9B-3P4, Emerging Technologies, Hydro-Québec Research Institute, 1800 Boulevard Lionel-Boulet, Varennes, Quebec, Canada J3X 1S1, and Department of Materials Science & Engineering, University of California, Los Angeles (UCLA), 405 Hilgard Avenue, Los Angeles, California 90095

Received November 24, 2003. Revised Manuscript Received April 1, 2004

A mesoporous tantalum oxide lithium fulleride composite was synthesized by solution intercalation of C_{60} into a prefabricated Li-TaTMS material and characterized by elemental analysis, X-ray diffraction (XRD), Raman spectroscopy, nitrogen adsorption−desorption, X-ray photoelectron spectroscopy (XPS), superconducting quantum interference device (SQUID) magnetometry, and solid-state ^{13}C and ^{7}Li NMR. The room conductivity measurements of Li fulleride material showed that this material was insulating, as opposed to previously synthesized K and Na based mesoporous Ta oxide fulleride composites with similar composition, which were semiconducting or metallic. Solid-state ^{7}Li NMR of this lithium composite exhibited a single Li environment. XPS measurements indicated an oxidation of the tantalum oxide walls had occurred upon intercalation of the fullerene ^{13}C NMR, and Raman measurements were consistent with one fulleride species in the pores. Electrochemical measurements revealed largely irreversible behavior upon intercalation/deintercalation of Li^+ into this material. This was attributed to the insulating nature of this composite impeding charge transport through the channels. In contrast, the corresponding Na fulleride intercalate showed reversible Li insertion, possibly due to enhanced charge transport through the semiconducting structure.

Introduction

Advances over the last 10 years in the nanofabrication of metal oxides have enabled researchers to control the porosity and shape of composite materials through use of liquid crystal phases, which act as templates around which the inorganic can nucleate and crystallize.[1−3] This strategy led to the development of M41S materials,[4−6] a class of silicas possessing pore sizes in the range of 20−100 Å, much larger than those available in conventional zeolites, which have pore sizes in the 5−15 Å range. The huge surface areas of up to 1400 m^2/g and large pores make these materials ideal for applications involving transport of large molecules to active sites within the pore structure. In 1996 J. Y. Ying reported the synthesis of Nb, Ta, and Ti analogues of these mesoporous materials,[7,8] the first example of stable transition-metal oxide based structures with controlled porosity in the 20−50 Å range. It was anticipated that these materials would offer many advantages in catalysis and design of electronic materials over mesoporous silicates, since the transition-metal oxide walls have available *d*-states which are an important feature in most electroactive and catalytic oxides. Subsequent work in our group demonstrated that the walls of the mesostructure function as a stoichiometric electron acceptor in reactions with alkali metal reagents.[9−11] This was the first example of a material with a porous structure having this property. Some Mn oxide channel materials act as Li acceptors but have a somewhat narrower window of structural stability upon alkali intercalation.[12] Because of the huge internal surface areas of up to 1000 m^2/g and the controlled pore structure, these mesoporous Nb, Ta, and Ti oxides

* To whom correspondence should be addressed. E-mail: danton@uwindsor.ca.
[†] University of Windsor.
[‡] Hydro-Québec Research Institute.
[§] University of Californi.

(1) Stein, A. *Adv. Mater.* **2003**, *15*, 736.
(2) Faul, C. F. J.; Antonietti, M. *Adv. Mater.* **2003**, *15*, 673.
(3) Lehn, J. M. *Supramolecular chemistry: Concepts and perspectives*; VCH: Weinheim, 1995.
(4) Kresge, C. T.; Leonowicz, M. E.; Roth, W. J.; Vartulli, J. C.; Beck, J. S. *Nature* **1992**, *359*, 710.
(5) Beck, J. S.; Vartuli, J. C.; Roth, W. J.; Leonowicz, M. E.; Kresge, C. T.; Schmitt, K. D.; Chu, C. T.-W.; Olson, D. H.; Shepard, E. W.; McCullen, S. B.; Higgins, J. B.; Schlenker, J. L. J. *J. Am. Chem. Soc.* **1992**, *114*, 10834.
(6) Tanev, P. N.; Chibwe, M.; Pinnavaia, T. J. *Nature* **1994**, *368*, 321.
(7) Antonelli, D. M.; Nakahira, A.; Ying, J. Y. *Inorg. Chem.* **1996**, *35*, 3126.
(8) Antonelli, D. M.; Ying, J. Y. *Angew. Chem. Int. Ed. Engl.* **1996**, *35*, 426.
(9) Vettraino, M.; Trudeau, M.; Antonelli, D. M. *Adv. Mater.* **2000**, *12*, 337.
(10) Vettraino, M.; Trudeau, M.; Antonelli, D. M. *Inorg. Chem.* **2001**, *40*, 2088.
(11) He, X.; Antonelli, D. M. *Angew. Chem. Int. Ed.* **2002**, *41*, 214.
(12) Brock, S. L.; Duan, N.; Tian, Z. R.; Giraldo, O.; Zhou, H.; Suib, S. L. *Chem. Mater.* **1998**, *10*, 2619.

10.1021/cm030548f CCC: $27.50
Published on Web 07/02/2004

represent ideal candidates for substrates in processes where fast diffusion through a large internal void space and redox activity are necessary features. They also offer the advantage of facile surface modification and manipulation of electronic properties by the introduction of various agents into the walls of the porous cavities.[11] Previous work in our group demonstrated that impregnation of these materials with alkali (Na, K) fullerides leads to conducting nanowires within the pores that have very different electronic properties than the bulk phases.[13−17] Because of the insulating nature of alkali metal intercalated mesoporous Nb, Ta, and Ti oxides, it can be reasoned that the conductivity is due mainly to charge transport through the alkali fulleride phase. However, a deeper investigation is needed in order to gain a more thorough understanding of charge-transfer behavior between the alkali metal, fullerene, and mesoporous transition-metal oxide host.

Electronic properties of alkali fullerides have attracted much attention since the first report of superconductivity in K_3C_{60} and subsequent reports of conducting films of C_{60} and C_{70} by alkali metal doping.[18,19] Molecular electronic states were suggested using Hückel molecular orbital calculation that the highest occupied molecular orbitals (HOMO) h_u level has 5 filled orbitals (10 electrons) and the lowest unoccupied molecular orbitals (LUMO) t_{1u} level holds 3 empty orbitals. The LUMO−HOMO gap is expected to be ∼2 eV and the LUMO bandwidth 0.5 eV.[20] Cyclic voltammograms of fullerenes C_{60} and C_{70} show similar features when dissolved in solvents such as CH_2Cl_2, THF, benzene, etc., exhibiting at maximum 6 peaks due to successive one-electron charge transfers. Their solution electrochemistry was reported to be complicated by different behaviors depending on solvent and cycling rate.[21−23] The electrochemistry of solid C_{60} is rather different from its solution phase counterpart. Electrochemical intercalation of lithium into solid C_{60} performed in an all-solid cell using the potentiostatic intermittent titration (PITT) technique showed that the insertion proceeds by several steps.[24] The first step is insertion of ∼0.5 mol Li per C_{60}, which opens the lattice structure to further, more favorable, insertion. The next steps, related to the insertion of up to 2 and 3 Li, were associated with octahedral and tetrahedral sites of the face centered cubic (*fcc*) lattice. Further insertion displayed a small shoulder and a successive larger peak, linked to the transition to body-centered tetragonal (*bct*) phase and shear-distorted *fcc* tetragonal phase.[24] As a result, structural and electronic properties of Li-metal doped fullerenes change in a complicated way, depending on charge transfer between fullerene and alkali metals and the number of Li centers involved. In the case of alkali fulleride-doped mesoporous Ta oxide composites, the charge transfer is expected to be more complex, owing to the presence of redox-active tantalum. To study this process in detail, electrochemistry is considered the most suitable tool, as it is able to closely scrutinize charge transfer over the course of lithium insertion/extraction of the composite.

In this paper we report the successful synthesis of Li fulleride doped mesoporous Ta oxide and investigate its electronic and electrochemical properties. Alkali doped materials are particularly interesting, because both the Ta oxide framework and the fulleride phase can act as an electron acceptor and alkali fullerides show a strong dependence of conductivity on level of electron filling in the t_{1u} band. The electronic properties of each component are examined by various techniques, including X-ray photoelectron spectroscopy (XPS), Raman spectroscopy, solid-state ^{13}C and ^{7}Li NMR, and magnetometry. Cyclic voltammetry is used to monitor charge-transfer phenomenon between redox-active components of the composites. Since it is conceivable that both the Ta oxide walls and the fulleride phase play an active roll in charge transport through the channels, a full electrochemical study on the intercalation and deintercalation of Li is presented, and a plausible interaction between the components is also discussed.

Experimental Section

Materials and Equipment. All chemicals unless otherwise stated were obtained from Aldrich. Samples of mesoporous tantalum oxide (Ta-TMS1) were synthesized according to the literature method[8] and used without further purification. Trimethylsilyl chloride was distilled over calcium hydride. In order to remove an excess of moisture and cap OH groups on the internal surface of the tantalum oxide mesostructure, which can interfere with the intercalation process by forming LiOH on the internal surface, mesoporous Ta oxide was dried at 100 °C overnight under vacuum and then stirred with excess trimethylsilyl chloride in dry ether for 12 h under nitrogen. Nitrogen adsorption and desorption data were collected on a Micromeritics ASAP 2010. X-ray diffraction (XRD) patterns (CuK_α) were recorded in a sealed glass capillary on a Bruker AXS D8-Discover diffractometer with 2D GADDS detector. All X-ray photoelectron spectroscopy (XPS) emissions were referenced to the Carbon C-(C,H) emission at 284.8 eV, and the data were obtained using a Physical Electronics PHI-5500 using charge neutralization. The room temperature conductivity measurements were recorded on a Jandel 4 point universal probe head combined with a Jandel resistivity unit. The equations used for calculating the resistivity were as follows: for pellets of <0.5 mm thickness:

$$\rho = \left(\frac{\pi}{\log n^2} \times \frac{V}{I}\right)t \qquad (1)$$

(13) Ye, B.; Trudeau, M.; Antonelli, D. M. *Adv. Mater.* **2001**, *12*, 29.
(14) Ye, B.; Trudeau, M.; Antonelli, D. M. *Adv. Mater.* **2001**, *13*, 561.
(15) Ye, B.; Trudeau, M.; Antonelli, D. M. *Chem. Mater.* **2001**, *13*, 2730.
(16) Ye, B.; Trudeau, M.; Antonelli, D. M. *Chem. Mater.* **2002**, *14*, 2774.
(17) Skadtchenko, B. O.; Trudeau, M.; Schurko, R. W.; Willans, M. J.; Antonelli, D. M. *Adv. Func. Mater.* **2003**, *13*, 671.
(18) Haddon, R. C.; Hebbard, A. F.; Rosseinsky, M. J.; Murphy, D. W.; Duclos, S. J.; Lyons, K. B.; Miller, B.; Rosamilia, J. M.; Fleming, R. M.; Kortan, A. R.; Glarum, S. H.; Makhija, A. V.; Muller, A. J.; Eick, R. H.; Zahurak, S. M.; Tycko, R.; Dabbagh, G.; Thiel, F. A. *Nature* **1991**, *350*, 320.
(19) Hebard, A. F.; Rosseinsky, M. J.; Haddon, R. C.; Murphy, D. W.; Glarum, S. H.; Palstra, T. T. M.; Ramirez, A. P.; Kortan, A. R. *Nature* **1991**, *350*, 600.
(20) Forro, L.; Mihaly, L. *Rep. Prog. Phys.* **2001**, *64*, 649.
(21) Allemand, P. M.; Srdanov, G.; Koch, A.; Khemani, K.; Wudl, F.; Rubin, Y.; Diederich, F.; Alvarez, M. M.; Anz, S. J.; Whetten, R. L. *J. Am. Chem. Soc.* **1991**, *113*, 1050.
(22) Jehoulet, C.; Bard, A. J.; Wudl, F. *J. Am. Chem. Soc.* **1991**, *113*, 5456.
(23) Compton, R. G.; Spackman, R. A.; Wellington, R. G.; Green, M. L. H.; Turner, J. *J. Electroanal. Chem.* **1992**, *327*, 337.
(24) Chabre, Y.; Djurado, D.; Armand, M.; Romanow, W. R.; Coustel, N.; McCauley, J. P.; Fischer, J. E.; Smith, A. B. *J. Am. Chem. Soc.* **1992**, *114*, 764.

For pellets of >0.5 mm thickness the following equation is used

$$\rho = 2\pi(S)\frac{V}{I}$$

where ρ = resistivity; $\pi/\log n^2$ = sheet resistivity; V = voltage; I = current; t = thickness of the pellet; and S = the spacing of the probes (0.1 cm). Measurements were done in triplicate in an inert atmosphere, allowing the system to stabilize for 30 min for each reading to ensure maximum reliability. Magnetic measurements were conducted on a Quantum Design superconducting quantum interference device (SQUID) magnetometer MPMS system with a 5 T magnet. Diamagnetic correction terms for the constituent elements were added to the data where appropriate.[25] Solid-state ^{7}Li and ^{13}C NMR spectra were obtained Spectral Data Services, Champagne, IL on a 363 MHz Oxford solenoid equipped with a Libra/NMR Kit Tecmag operating system. Doty Scientific 7 mm probe was used for all experiments. Samples were ground into a fine powder under an inert atmosphere and tightly packed into Si_3N_4 rotors, which were sealed with airtight kel-F end caps. ^{7}Li chemical shifts were referenced to a 1 M solution of LiCl (δ_{iso} = 0.0 ppm). ^{7}Li MAS NMR spectrum was acquired with a spinning speed of 8 kHz, recycle delay was 4 s, and between 100 scans was acquired. For ^{13}C NMR glycine was used as a secondary reference to TMS ($\delta_{iso}(^{13}C)$) = 0.0 ppm. Single-pulse ^{13}C MAS NMR and $^{13}C\{^1H\}$ CPMAS experiments, with a recycle delays of 9 s, spinning speed of 8 kHz, and with and without decoupling, were conducted. The number of transients collected varied from 600 to 786. The Raman spectra were recorded on a Renishaw Ramascope using a Renishaw 514 nm Diode Laser System. All elemental analysis data were conducted under an inert atmosphere by Galbraith Laboratories, 2323 Sycamore Drive, Knoxville, TN 37921-1700. Metal analysis was conducted by inductively coupled plasma (ICP) techniques. The electrochemical cell was set up with a conventional three electrode configuration. The reference and counter electrodes were lithium metal foils (Aldrich 99.99%). Therefore, all potentials are noted with respect to Li^+/Li. Electrolyte was 1 M $LiClO_4$ in propylene carbonate (PC) or dimethyl carbonate (DMC). The working electrode was made by deposition of propylene carbonate (Aldrich 99+ %) solution containing active material (tantalum oxide-alkali metal fulleride composite) and polyvinyldiflouride (PVdF) with 9:1 mass ratio. The electrodes were dried at 130 °C under vacuum overnight. Cyclic voltammetry was performed in three ranges: 1.5−3.5 V, 0.5−3.5 V, 0.005−3.5 V. More detailed conditions are described in the Results and Discussion section.

Synthesis. To a benzene suspension of Ta-TMS1 previously reduced with 1.0 molar equiv of lithium naphthalene with respect to Ta was added excess C_{60}. After several days of stirring to ensure complete absorption of the fullerene, the material was collected by suction filtration and washed several times with THF. The material was dried in vacuo at 10^{-3} Torr on a Schlenk line until all condensable volatiles had been removed. This solid was characterized by Raman, XPS, and elemental analysis to ensure sample quality before proceeding with SQUID and conductivity studies. From the elemental analysis data the molecular weight of Li fulleride composite of 373.87 g/mol was calculated. The Na-fulleride mesoporous Ta oxide material was prepared as described previously.[17]

Results and Discussion

Synthesis and Characterization. In previous work mesoporous oxide composites of Na and K fullerides were synthesized by treating a suspension of the oxide in THF with a THF solution of the corresponding alkali fulleride. To synthesize Li analogues of these materials it thus seemed reasonable to start with mesoporous Ta oxide and a soluble Li fulleride source. However, initial attempts to prepare Li fullerides by conventional thermal methods[13,17] proved difficult as Li_3C_{60} cannot be obtained phase pure without the use of elevated temperature in conjunction with a high-pressure apparatus.[26] Attempts to synthesize stock solutions of Li_3C_{60} in THF by treatment of C_{60} with Li naphthalene or butyllithium led only to formation of insoluble products which could not be used in intercalation reactions. Owing to these difficulties, materials with variable Li:C_{60} ratios were prepared by a second route involving treatment of mesoporous Ta oxide reduced with 1.0 equiv of Li-naphthalene[10] with excess C_{60} in benzene. This route proved effective in the synthesis of potassium fulleride composites of mesoporous niobium oxide[16] and relies on the unique ability of the alkylated mesostructure to reduce the fullerene, rather than using an alkylated fulleride to reduce the mesostructure. This route has the advantage that materials of different Li and C_{60} ratios can readily be made by simply varying the quantities of these two dopants. Over the course of our work we discovered that materials treated with smaller amounts of Li are less effective reducing agents and absorb less C_{60}, suggesting that the intercalation of the fullerene is a process driven by electron transfer from the mesostructure.[10] This is in accord with previous work in our group on potassium fulleride mesoporous niobium oxide composites.[13,14] For the sake of simplicity, we chose in this study to focus on the material with 1.0 equiv of Li with respect to Ta and a maximum amount of C_{60}.

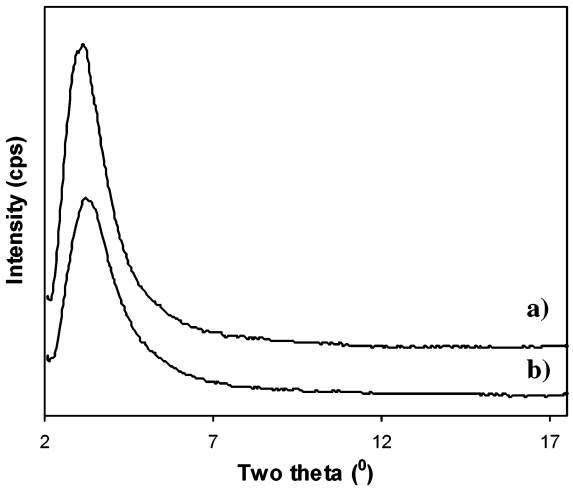

Figure 1. XRD of (a) mesoporous Ta oxide with 22 Å pore size and (b) a sample from (a) treated with 1.0 molar equiv of Li-naphthalene with respect to Ta, followed by impregnation with C_{60}.

Figure 1 shows the XRD patterns for the untreated mesoporous Ta oxide and the material after treatment with Li naphthalene and C_{60}. The main XRD peak falls at ca. 28 Å in both materials, demonstrating that the mesostructure has been retained and was relatively unaffected by impregnation. Figure 2 shows the nitrogen adsorption/desorption isotherms of these two materials. The volume of nitrogen adsorbed at any given

(25) Cheetham, A. K.; Day, P. *Solid State Chemistry Techniques*; Oxford University Press: Oxford, UK, 1998.

(26) Mitronova, G. U.; Savchenkova, A. P.; Mayorova, A. F.; Mudretsova, S. N.; Avdeev, V. V. *Russ. Ser. Chem.* **1996**, *48*, 491.

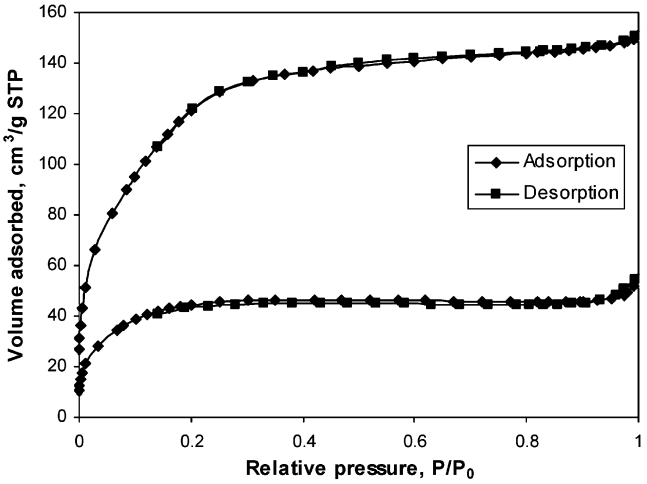

Figure 2. Nitrogen adsorption/desorption isotherms of materials: from Figure 1a (top) and from Figure 1b (bottom).

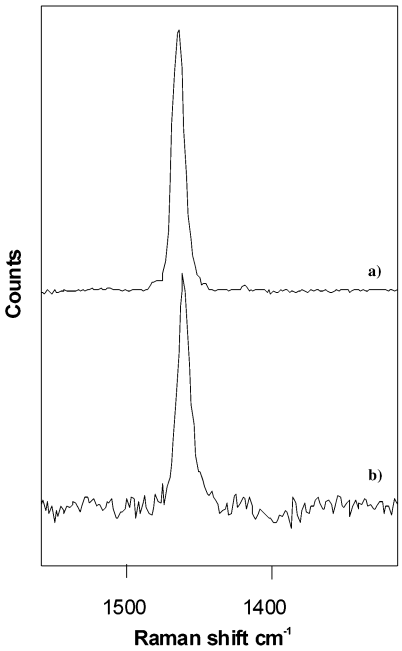

Figure 3. Raman spectra of (a) pure C_{60} and (b) composite from Figure 1b.

P/P_0 has decreased, consistent with partial filling of the channels with fullerene units. The BET (Brunauer−Emmet−Teller) surface area has dropped from 469 m^2/g in mesoporous Ta-TMS to 163 m^2/g in the Li fulleride intercalate, while the HK (Horvath−Kawazoe) pore size decreased from 23 Å to 18 Å, respectively. Figure 3 shows the Raman spectrum of this new composite, displaying an A_g mode at 1462 cm^{-1}. By comparison with the spectrum of pure C_{60}, which exhibits an A_g mode at 1464 cm^{-1}, it appears that no visible reduction of C_{60} has occurred. The slight difference between these two values was attributed to the accuracy of Raman spectroscopy, which is within ±2 cm^{-1}. The absence of visible reduction of C_{60} in this composite was further confirmed by the NMR data discussed below. The elemental analysis of this material gave 23.2% C and 1.24% H as compared to 3.71% C and 1.26% H in the starting mesoporous Ta oxide. The percentage of Li and Ta in the composite material was 1.68 and 48.41%, respectively, giving a molar ratio of Li/Ta/C as 0.79/1/7.23. This provides a Li/Ta/C_{60} ratio of 0.79/1/0.12. Solid-state ^{7}Li MAS NMR experiments (Figure 4a) show only one broad Li resonance similar to the resonance observed in the material prior to treatment with C_{60}. Since there is a narrow range of shifts in ^{7}Li NMR, assigning exact Li environments on the basis of shift alone can be misleading. For this reason, a complete study of the ^{7}Li NMR in Li-reduced mesoporous Ti oxide is currently being completed by our group.[27] The ^{13}C CPMAS NMR spectrum of this material (Figure 4b) shows a variety of carbon species with three distinct resonances at around 24, 72, and 143 ppm. Broad resonances at 24 and 72 ppm are assigned to THF used during the preparation of mesoporous material. The narrow resonance centered at 143 ppm can be attributed to a single C_{60} species and is almost coincident to the resonance for pure fullerene,[28−30] consistent with the Raman measurements. The absence of any other resonances within 140−170 ppm range where chemical shifts for multiple C_{60}^{n-} species are normally observed further indicates that no visible reduction of the fullerene has occurred.

The XPS Ta 4*f* region of this Li fulleride composite (Figure 5c) displays 7/2, 5/2 emissions at 26.9 eV and 28.7 eV, respectively. These are virtually identical to those observed in the spectrum of pure mesoporous Ta oxide (26.9 and 28.7 eV), shown in Figure 5a for the sake of comparison. These emissions appear at slightly higher binding energies than those observed in the spectrum of the materials reduced with 1 equiv of Li-naphthalene prior to treatment with fullerene (26.7 and 28.5 eV), indicating that some electron density has been donated from the walls of the Ta oxide mesostructure to the fullerene phase. This is consistent with Li transfer to the fulleride phase. The lack of observable change in peak position with respect to pure unreduced C_{60} in Raman or ^{13}C NMR spectra is not unexpected, because Li does not give complete charge transfer into the t_{1u} band of C_{60}. This has been commented on before by Kosaka et al.[31] and generally leads to some spectroscopic ambiguity in assigning exact values to the oxidation state of Li fullerides. For example, Li_3CsC_{60} has a Raman shift corresponding to $n \approx 3$, where n is oxidation state of fulleride.[31] The difference between Li and other alkali metals in this system is further born out in the XPS spectra of alkali metal reduced mesoporous Ta oxide. There is relatively little change in the Ta 4*f* emissions on reduction with 1.0 equiv of Li (0.2 eV); however, mesoporous Ta oxide Na-fulleride composites show a range of over 2 eV in the Ta 4*f* region, depending on the Na loading level up to 1.0 equiv. Thus, the relative oxidation states of fulleride and Ta oxide in the Li composites are not as clearly defined from a spectroscopic standpoint as they are for the Na−Ta composites studied previously. In previous work detailing the trend in Nb 3*d* binding energies with reduction

(27) Vettraino, M.; Loo, A.; Schurko, R. W.; Antonelli, D. M. Unpublished results.
(28) Tanigaki, K.; Prassides, K. *J. Mater. Chem.* **1995**, *5*, 1515.
(29) Tanigaki, K.; Hirosawa, I.; Manako, T.; Mizuki, J.-I.; Ebbesen, T. W.; Prassides, K. *The Electrochemical Society Proceedings Series PV 94-24*; Pennington, NJ, 1994; p 546.
(30) Tycko, R.; Haddon, R. C.; Dabbagh, G.; Glarum, S. H.; Douglass, D. C.; Mujsce, A. M. *J. Phys. Chem.* **1991**, *95*, 518.
(31) Kosaka, M.; Tanigaki, K.; Prassides, K.; Margedonna, S.; Lappas, A.; Brown, C. M.; Fitch, A. N. *Phys. Rev. B* **1999**, *59*, 6628.

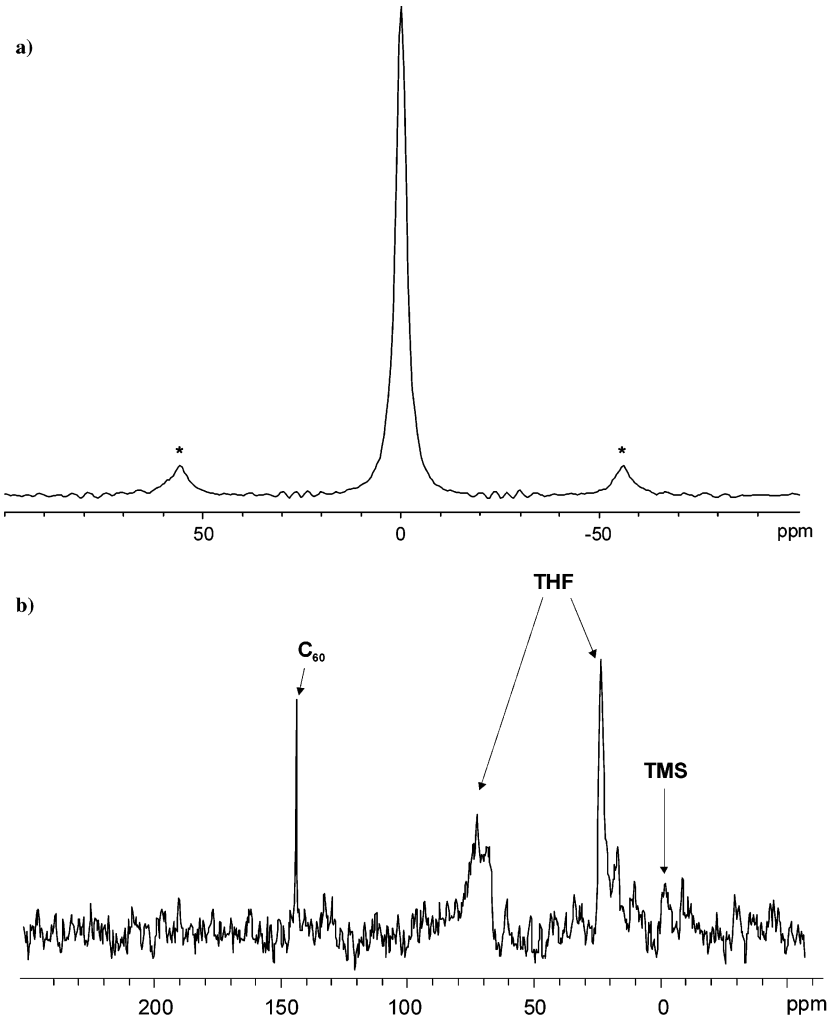

Figure 4. (a) ^{7}Li MAS NMR of composite from Figure 1b and (b) ^{13}C MAS NMR of composite from Figure 1b. TMS here refers to trimethylsilyl.

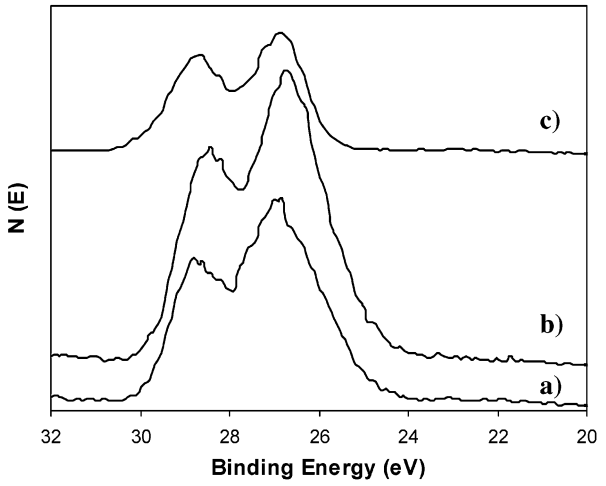

Figure 5. XPS spectrum showing Ta 4f region of (a) mesoporous Ta oxide, (b) mesoporous Ta oxide reduced with 1.0 molar equiv of Li-naphthalene with respect to Ta, and (c) material (b) after impregnation with C_{60}.

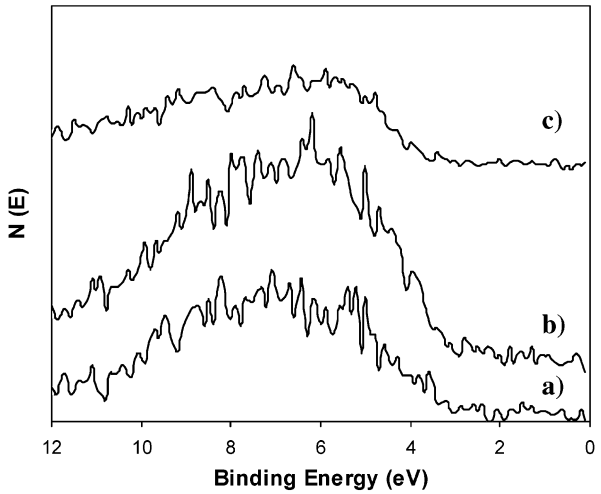

Figure 6. XPS spectrum showing region near Fermi level of (a) mesoporous Ta oxide, (b) mesoporous Ta oxide reduced with 1.0 molar equiv of Li-naphthalene with respect to Ta, and (c) material (b) after impregnation with C_{60}.

by 1.0 equiv of alkali metal (Li, Na, K, Rb, Cs), the smaller alkali metals consistently gave higher Nb 3*d* binding energies (0.5 eV per row) than the larger alkali metals.[10] This is consistent with a lower degree of charge transfer to the framework in those materials reduced with smaller alkali metals.[16,17] These differences can be accounted for by the differences in size, electronegativity, and electron affinity between the alkali metals.

The region near the Fermi level is shown in Figure 6 and resembles that of analogous composites studied in our group showing a noticeable but broad O *sp* emission

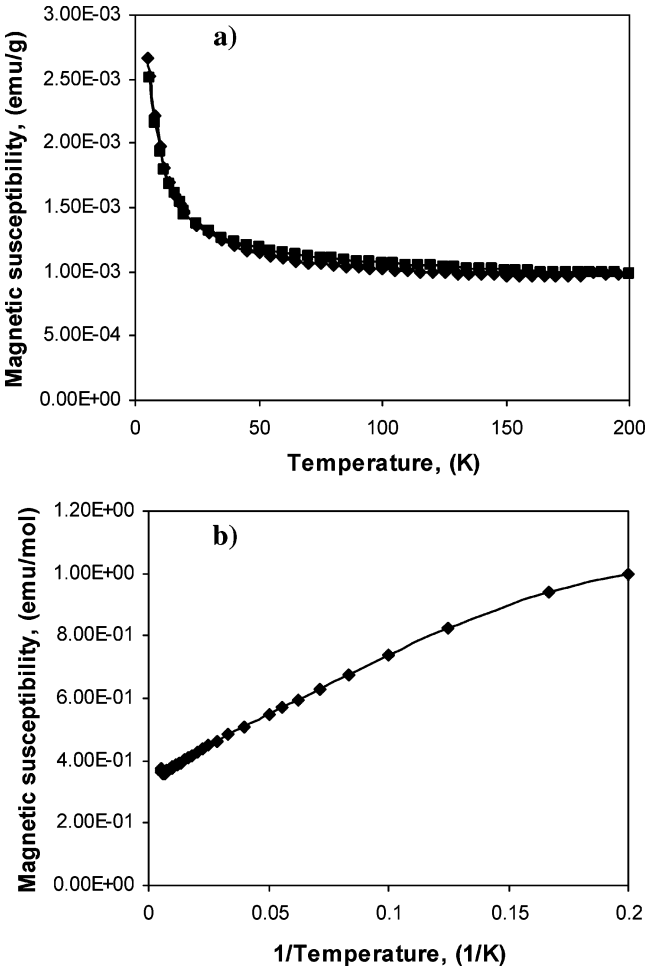

Figure 7. Plots of (a) magnetic susceptibility versus temperature and (b) normalized molar magnetic susceptibility versus inverse temperature of sample from Figure 1b.

and no visible 5*d* states expected from a partially populated framework impurity band. The lack of an observable *d* emission near the Fermi level is common in reduced mesoporous oxides studied by our group and can be attributed to the broad dispersion of *d* states in the amorphous wall structure or, perhaps in this case, an incomplete charge transfer from the Li to the Ta *5d* band.

The conductivity of the Li fulleride composite as measured by the four-point technique at room temperature provided values of $<10^{-7}$ ohm^{-1} cm^{-1}. This behavior contrasts strongly to that observed in the Na and K analogues. In previous work the semiconducting-to-metallic nature of a broad range of Na- and K-reduced mesoporous Nb and Ta oxides was attributed to reduced fullerene species in the pores. In these one-dimensional mesoporous oxide alkali fulleride (A_nC_{60}) composites studied in our group, $n = 0.5$ and $n = 2.5$ are always semiconductors, $n = 3$ is always insulating, and $n = 4$ is either a semimetal or a metal. The different conductivity of the Li material once again underscores the difference between this alkali metal and its larger congeners and further warrants detailed electrochemical investigation.

The results of Superconducting Quantum Interference Detector (SQUID) magnetometer measurements conducted on Li composite over the temperature range 4−200 K at 500 G are shown in Figure 7. The plot of χ vs T (Figure 7a) indicates that this material has a strong temperature independent paramagnetism term of 3.5 $\times 10^{-1}$ emu/mol, which can be attributed to Van Vleck paramagnetism, since Pauli paramagnetism is not expected on the basis of the lack of metallic behavior. The SQUID χ vs $1/T$ plot is shown in Figure 7b and indicates that this material obeys the Curie Law from 10 to 140 K. Below this temperature the magnetization drops off, consistent with a small degree of spin glass behavior in these materials. The Curie constant can be calculated from this plot as 4.02 emu*K/mol with a $\mu_{eff} = 1.724\ \mu_B$, consistent with approximately one unpaired electron per Ta. The plot of $1/\chi$ vs T was not linear, demonstrating that the Curie Weiss law does not provide a better fit for these data.

All other mesoporous oxide alkali fulleride composites, studied before,[13−17] could be further reduced by addition of alkali naphthalene reagents in THF. This allowed us to chart the dependence of conductivity and magnetic behavior on alkali metal loading level and absolute composition and relate this to the physical properties of bulk alkali fullerides at similar levels of reduction. The most surprising result of these studies were that the $n = 3$ state was insulating and the $n = 4$ state was metallic or a semimetal, the opposite of what is observed (but not expected from calculations)[18,32−34] in the bulk materials. Attempts to reduce this new composite with Li-naphthalene in THF were unsuccessful and led to no observable reaction. Since Li naphthalene is a strong enough reagent to reduce either mesoporous Ta oxide or C_{60}, the fullerene units in these composites are likely blocking the pores and preventing reduction within the channels. This suggests that electron transfer from the alkali naphthalene reagent to the fulleride in the related composites studied previously is strongly dependent on conductivity through the channels, because these materials are likely to have similar steric restrictions in the pores as compared to the Li materials. Thus alkyl naphthalene reduction in these materials likely occurs via reaction on the outside of the channels and subsequent charge transport through the channels (hindered in the Li system by its insulating nature), rather than movement of the alkali naphthalene reagent through the pores directly to the active site. To further explore the mechanism of charge mobility in this system, electrochemical studies were conducted.

Electrochemistry. Since the lithium fulleride composites are insulating and the sodium fulleride composites are semiconductors, we expect very different electrochemical behaviors. Alkali-fulleride-intercalated mesoporous tantalum oxide composite has two active components for electrochemistry: fullerene and tantalum. Tantalum oxide is known to have very low reduction potential, which is accompanied by intercalation of lithium ions from lithium-based nonaqueous electrolytes.[35,36] As stated earlier, electrochemistry of solid C_{60} is complex, and its cyclic voltammogram has several

(32) Lof, R. W.; van Veenendaal, M. A.; Koopmans, B.; Jonkman, H. T.; Sawatzky, G. A. *Phys. Rev. Lett.* **1992**, *68*, 3924.
(33) Mott, N. F. *Metal−Insulator Transition*, 2nd ed.; Taylor & Francis: London, 1999.
(34) Rosseinsky, M. J. *Chem. Mater.* **1998**, *10*, 2665.
(35) Fu, Z. W.; Qin, Q. Z. *Electrochem. Solid-State Lett.* **1999**, *2*, 600.
(36) Fu, Z. W.; Qin, Q. Z. *Electrochem. Solid-State Lett.* **2000**, *147*, 4610.

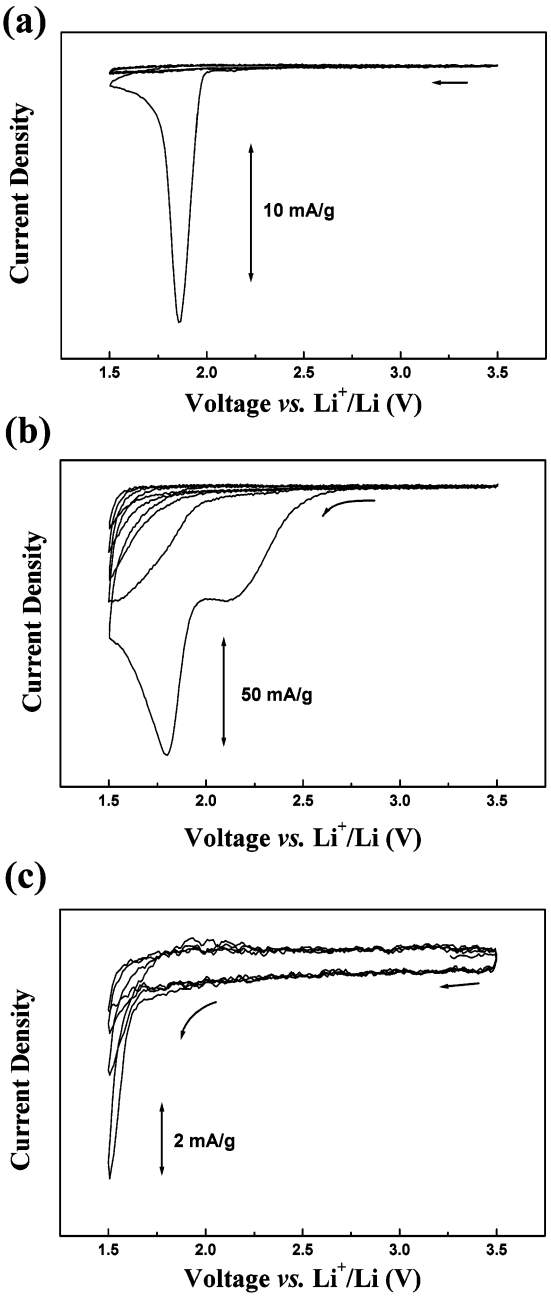

Figure 8. Cyclic voltammograms for (a) composite from Figure 1b, (b) sodium fulleride-tantalum oxide composite, and (c) mesoporous tantalum oxide. Voltage was cycled at 1 mV/s between 1.5 and 3.5 V, and propylene carbonate was used as a solvent.

peaks related to different sites and phase transition at high insertion ratio.[20−24] Because of this, cyclic voltammetry was conducted under various conditions, changing the voltage range and cycling rate.

First, the voltage range was set to 1.5−3.5 V, and the corresponding voltammograms are shown in Figure 8. The lithium fulleride-tantalum oxide composite showed a large irreversible peak around 1.9 V, whereas two peaks can be observed around 2.1 and 1.8 V for the sodium analogue, which decrease with continued cycling. In contrast, mesoporous tantalum oxide alone showed a small irreversible peak at 1.5 V, which indicates the electrochemical behavior in the composites originates from the fullerene component. Chabre et al. demonstrated that electrochemical lithium intercalation

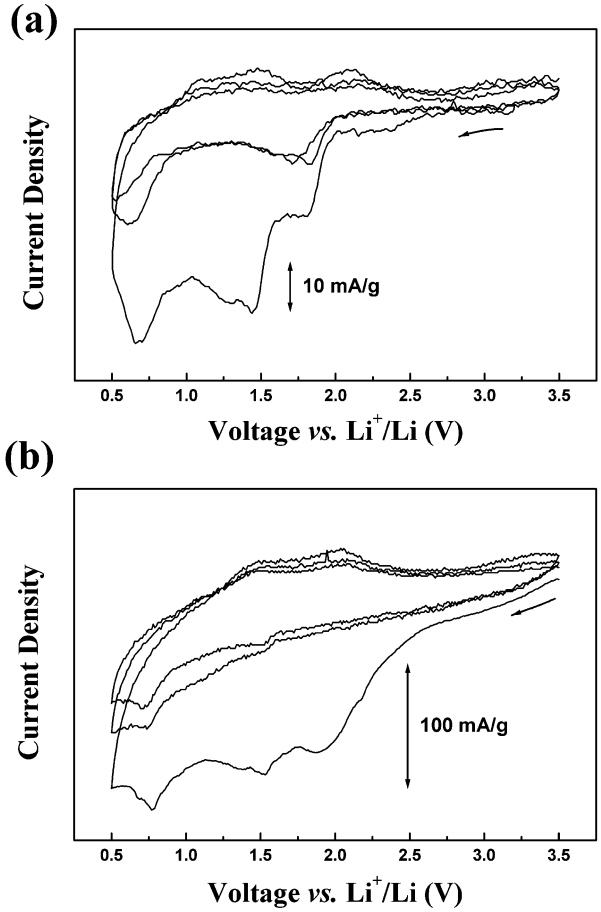

Figure 9. Cyclic voltammograms for (a) composite from Figure 1b and (b) sodium fulleride-tantalum oxide composite. Voltage was cycled at 1 mV/s three times between 0.5 and 3.5 V, and dimethyl carbonate was used as a solvent.

into C_{60} films occurs at 2.3, 1.9, 1.5, 1.0, and 0.8 V, where the first three peaks are related to the insertion into octahedral and tetrahedral sites in the *fcc* lattice, and the last two are associated with a phase transition to *bct* and *bcc* phases, respectively.[24] It was also reported that the first three reactions are reversible, but the phase transition to *bct* phase is not. In our experiments, only one (Li-based composite) or two (Na-based composite) peaks can be observed (Figure 8a,b), and the 2.3 V-peak is absent. The reason for this is possibly because the space available in the Ta oxide channels is too narrow for the fullerene molecules to develop strong lattice interactions, and that the small amount of alkali metals residing in the as-prepared composites has already opened the lattice prior to electrochemical Li insertion. There is, consequently, no 2.3 V-peak related to lattice-opening. In addition, the absence of reversibility may result from the strong interaction between inserted lithium ions and tantalum oxide. It should be mentioned that the exact chemical ratio of Li interacting with fullerene is difficult to estimate because of the presence of reducible Ta framework which can compete for Li.

Next, the voltage range was enlarged to 0.5−3.5 V (Figure 9). Both samples showed two new cathodic peaks around 1.5 and 0.75 V. The 1.5 V-peak is very diminutive for the lithium-based sample but is more noticeable for the sodium-based composite. Even though the two composites showed a large difference in the

current density (~30 mA/g for the Li-based material and 150 mA/g for the Na-based one), both samples exhibit reversibility for the 1.5 V-peak. Such difference in current density can be related in part to the different conductivity of the materials; however, factors associated with the transport of lithium ions through the mesoporous structure may also be at play. In light of these observations, the difference of the interaction force between inserted lithium and the host material may also contribute to the degree of reversibility. The 0.75 V-peak exhibits some reversibility for both samples. About two-thirds of the capacity was lost after the first cycle. It should be noted that the 1.5 V-peak is not prominent for Li fulleride in the voltage range 1.5−3.5 V (Figure 8a); however, in a range of 0.5−3.5 V it narrows and becomes more evident (Figure 9a). The reason for this is not understood but could be due to the different electrolytes used during the measurements (a PC-based electrolyte was used to perform electrochemistry measurements presented in Figure 8 and a DMC-based electrolyte was used for all other measurements). Generally, PC and DMC show similar behavior as nonaqueous polar solvents. Even though the first cycle of the Li-composite is different for the 1.5 V-peak, its position remains the same in both cases and it becomes entirely the same after the second cycle. This suggests that a kind of passivating layer forms in the first cycle for the DMC-based measurements.

Further expansion of the voltage scope to 0.005−3.5 V after cycling between 0.5 and 3.5 V (Figure 10) showed a large difference between the lithium-based sample and sodium-based materials. The lithium-based sample showed two large irreversible peaks, after which no further peaks were evident. In contrast, the sodium-based composite displayed a large featureless cathodic current increase. This rather irreversible behavior is possibly due to the extraction and replacement of Na by Li, since standard reduction potential of Na (~2.71 V vs SHE) is higher than that of Li (~3.04 V vs SHE). Pulsed-laser-deposited amorphous Ta_2O_5 exhibited similar electrochemical behavior.[35,36] This is in good agreement with the ^{23}Na NMR results where lithium ions go into the tantalum oxide lattice at low potential. For comparison, the cyclic voltammogram of pristine mesoporous tantalum oxide is also presented. Besides an irreversible peak around 0 V, it shows a slightly reversible peak at around 0.75 V. Therefore, the mesoporous tantalum oxide host has somewhat different electrochemical characteristics from the corresponding amorphous analogue, probably due to its mesostructure. The cathodic peaks presented in Figure 8a and 10a are sharp, while the other peaks (Figures 8b, 9a,b, 10b,c) are not. The appearance of such inferred peaks is most likely related to a fast one-step reaction, while the broad and less intense peaks are due to gradual diffusion. The large surface area may contribute to surface-site related current, which is somewhat different from the bulk-site related one. This is evident in the case of the 0.75 V-peak in the pristine Ta_2O_5 which is reversible and not obvious for most amorphous tantalum oxides. This peak could be assigned to the surface sites related to the mesoporous structure. More exhaustive investigation is necessary to elucidate all the detailed features of the electrochemistry of these mesoporous composites.

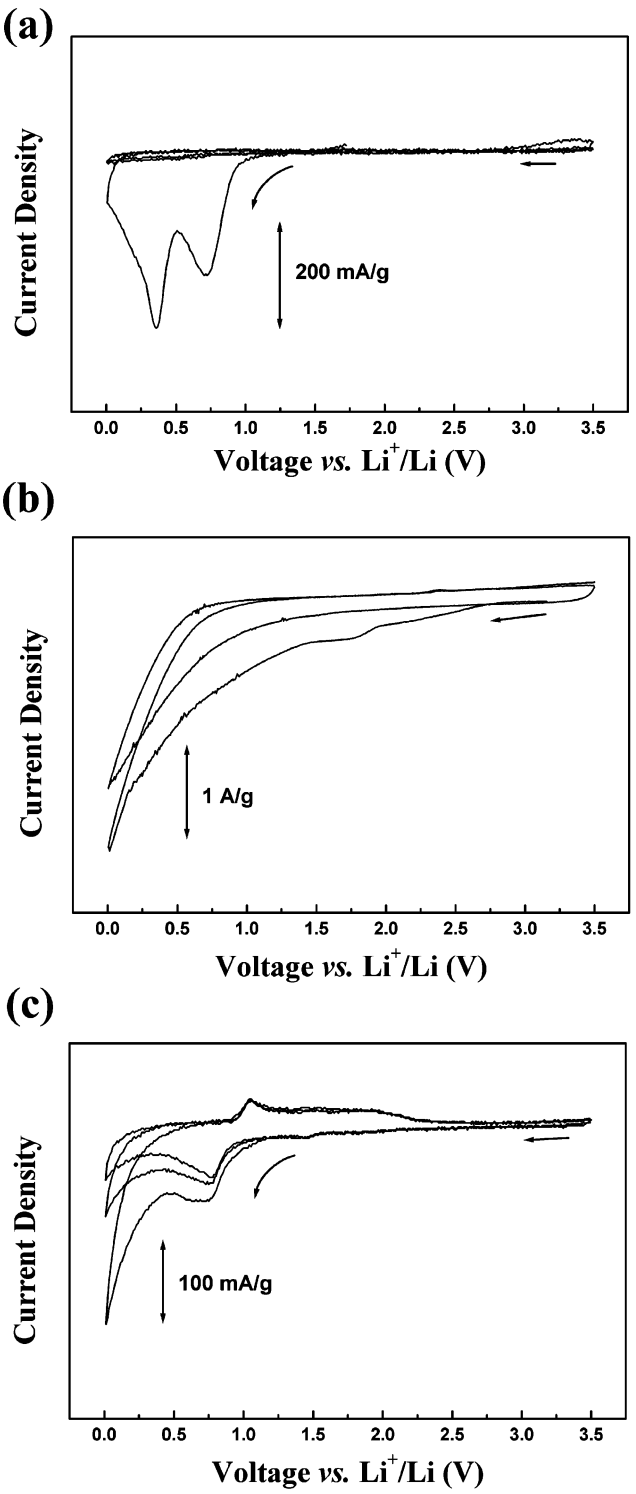

Figure 10. Cyclic voltammograms for (a) composite from Figure 1b, (b) sodium fulleride-tantalum oxide composite, and (c) mesoporous tantalum oxide. Voltage was cycled at 1 mV/s between 0.005 and 3.5 V, and dimethyl carbonate was used as a solvent.

Based on these results, Li insertion into the fulleride composites is irreversible except for the ~1.5 V peak of Na-based composite. The appearance of a reversible peak at ~0.75 V in all composite materials as well as in pristine mesoporous Ta oxide is not completely understood but could be related to surface sites in the mesoporous structure. The low level of reversibility in the Li-based composite is likely related to its insulating

nature which possibly results from the strong interaction between inserted lithium and the walls of mesostructure. In contrast to the electrochemical behavior in the Li fulleride composites, the insertion of Li into pristine mesoporous tantalum oxide showed reasonable reversibility. The fullerene units in the pores only facilitate reversible electron transfer when they form an accessible conductivity pathway through the channels. Otherwise, they only serve to hinder charge transport through the material for steric reasons. However, the mechanism of charge transfer through the channels is still ambiguous, and there are many cases in zeolites in which reversible electrochemistry occurs at the surface of an insulating grain and charge transfer occurs via electrolyte counteractions through the porous system.[37,38] This mechanism may also be operative in this system. To further delineate the nature of ion mobility in this system, a detailed ^{7}Li NMR study on Li-reduced mesoporous Ti and Ta oxides, relating the electrochemical data presented here to the inserted Li sites, is forthcoming.[27]

Conclusion

Lithium fulleride composites of mesoporous Ta oxide were synthesized by treatment of Li-reduced mesoporous Ta oxide with C_{60} in benzene and the material characterized by Raman, XPS, XRD, nitrogen adsorption, elemental analysis, ^{13}C- and ^{7}Li NMR, and SQUID magnetometry. In contrast to analogous K and Na fulleride composites of similar composition, these materials were insulating and could not be further reduced by chemical means. Electrochemical studies were conducted to compare Li insertion/deinsertion behaviors of this composite to previously synthesized Na fulleride mesoporous Ta oxide composite and to pristine mesoporous tantalum oxide. The results of these studies showed that Li insertion into the fullerene composites is rather irreversible in the Li material and more reversible in the more highly conducting Na-analogue. Comparisons with the Li insertion into pristine mesoporous Ta oxide suggest that fullerene doping adversely affects charge transfer unless the fullerene chains are highly conducting.

Acknowledgment. The Petroleum Research Fund administered by the American Chemical Society is thanked for funding. NSERC and the Ontario Premiere's Research Excellence Program are also thanked for financial support.

CM030548F

(37) Rolison, D. R. *Stud. Surf. Sci. Catal.* **1994**, *85*, 543.
(38) Dutta, P. K.; Ledney, M. *Prog. Inorg. Chem.* **1997**, *44*, 209.